JACS
JOURNAL OF THE AMERICAN CHEMICAL SOCIETY
Article
pubs.acs.org/JACS

Pt(IV) Prodrugs Designed to Bind Non-Covalently to Human Serum Albumin for Drug Delivery

Yao-Rong Zheng, Kogularamanan Suntharalingam, Timothy C. Johnstone, Hyunsuk Yoo, Wei Lin, Jamar G. Brooks, and Stephen J. Lippard*

Department of Chemistry, Massachusetts Institute of Technology, Cambridge, Massachusetts 02139, United States

Supporting Information

ABSTRACT: Albumin is the most abundant protein in human serum and drugs that are administered intravenously inevitably interact with it. We present here a series of platinum(IV) prodrugs designed specifically to enhance interaction with human serum albumin (HSA) for drug delivery. This goal is achieved by asymmetrically functionalizing the axial ligands of the prodrug so as to mimic the overall features of a fatty acid. Systematic variation of the length of the aliphatic tail tunes the cellular uptake and, consequently, the cytotoxicity of *cis,cis,trans*-[$Pt(NH_3)_2Cl_2(O_2CCH_2CH_2COOH)$-(OCONHR)], **4**, where R is a linear alkyl group. Investigation of an analogue bearing a fluorophore conjugated to the succinate ligand confirmed that these compounds are reduced by biological reductants with loss of the axial ligands. Intracellular release of cisplatin from **4** was further confirmed by observing the characteristic effects of cisplatin on the cell cycle and morphology following treatment with the prodrug. The most potent member of series **4**, for which R is a hexadecyl chain, interacts with HSA in a 1:1 stoichiometry to form the platinum-protein complex **7**. The interaction is non-covalent and extraction with octanol completely removes the prodrug from an aqueous solution of HSA. Construct **7** is robust and can be isolated following fast protein liquid chromatography. The nature of the tight interaction was investigated computationally, and these studies suggest that the prodrug is buried below the surface of the protein. Consequently, complexation to HSA is able to reduce the rate of reduction of the prodrug by ascorbate. The lead compound from series **4** also exhibited significant stability in whole human blood, attributed to its interaction with HSA. This favorable redox profile, in conjunction with the established nonimmunogenicity, biocompatibility, and enhanced tumor accumulation of HSA, produces a system that holds significant therapeutic potential.

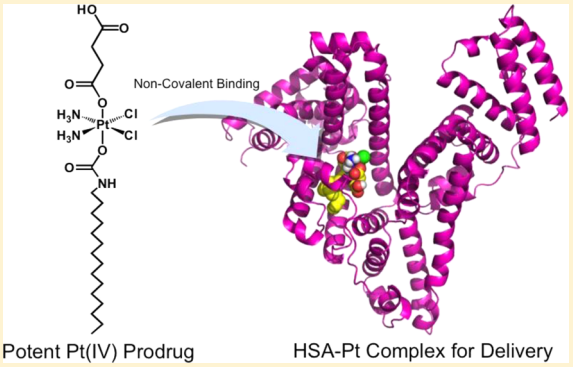

INTRODUCTION

The FDA-approved platinum-based drugs cisplatin, carboplatin, and oxaliplatin are widely used in the clinical treatment of cancer.[1,2] Cisplatin and carboplatin are extensively employed to treat ovarian, lung, head, and neck cancers, whereas oxaliplatin is marketed for the treatment of colorectal cancer.[3] The anticancer activity of these compounds arises from their ability to form intra- and interstrand cross-links on DNA via coordination of the N7 atoms of purine bases to the platinum center.[1,4] One of the prominent effects of these cross-links is inhibition of DNA and RNA polymerases, which, when stalled, can initiate a signaling cascade that leads to cell death.[5] Only a small portion of the platinum administered to a patient platinates the DNA of cancer cells, and reaction with off-target nucleophiles leads to toxic side effects including nephrotoxicity, myelosuppression, peripheral neuropathy, ototoxicity, and nausea.[2,6]

One strategy to improve the therapeutic index and decrease side effects that has received a significant amount of attention is the Pt(IV) prodrug approach.[7−10] Pt(IV) prodrugs are typically prepared by chemical oxidation of an active square-planar Pt(II) species, which adds two so-called "axial" ligands to the metal center. The resulting pseudo-octahedral Pt(IV) complex is more inert to ligand substitution than the parent Pt(II) complex and consequently reduces the extent of platinum sequestration and deactivation en route to the tumor cell. Within the reducing environment of the cancer cell, the Pt(IV) center is converted to Pt(II) with release of two ligands and regeneration of the active square-planar Pt(II) complex. Owing to the activation step required for Pt(IV) complexes, they generally exhibit less potency and toxicity than their Pt(II) counterparts. In addition to kinetic inertness, one of the great advantages of the Pt(IV) prodrug approach is that the axial ligands can be used to tune the physical and chemical properties of the complex without altering the structure of the active pharmacophore that is ultimately released. In this way, axial ligands have been used to tune the lipophilicity and redox potential of Pt(IV) complexes with the aim of altering cellular uptake and the kinetics of reductive activation.[11−14] In an alternative approach, bioactive ligands can be attached to the axial positions of a Pt(IV) complex to impart targeting[15,16] or

Received: April 16, 2014
Published: June 6, 2014

   dx.doi.org/10.1021/ja5038269 | J. Am. Chem. Soc. 2014, 136, 8790−8798

additional biological activity.[17−21] Axial ligands can also be chosen to facilitate delivery of platinum complexes by a nanosized object. Hydrophobic carboxylates have proved valuable for delivery of platinum complexes within the core of nanoparticles formed from amphiphilic block copolymers[22−25] or within carbon nanotubes.[26] A significant impediment to the clinical progression of Pt(IV) prodrugs is premature reduction in the bloodstream,[27,28] and nanodelivery constructs such as those described above may help protect the platinum center as it travels to the tumor.

In this paper, we present the development of a series of Pt(IV) complexes designed to exploit an endogenous protein, human serum albumin (HSA), as a delivery device. A key aspect in our design was the generation of compounds that mimic the amphiphilic structure of fatty acids. This goal was accomplished by preparing an asymmetrically functionalized cisplatin prodrug in which one axial ligand is succinate and the other an unbranched aliphatic carbamate (Scheme 1). We

Scheme 1. Synthetic Route for Preparing 4a−e from cisplatin: (a) 30% H_2O_2, 50 °C; (b) succinic anhydride, anhydrous DMSO, R.T.; (c) R−N═C═O, anhydrous DMF, R.T

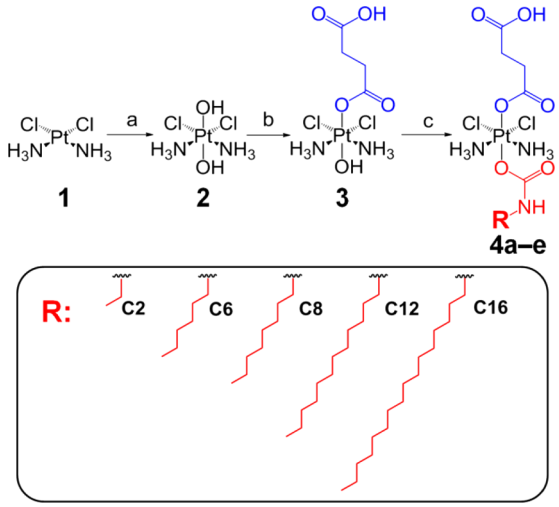

hypothesized that this structural motif would facilitate association of **4** with HSA. HSA is the single most abundant protein in human blood, present at concentrations of 34−54 g L^{-1},[29] and it serves a wide variety of functions ranging from the maintenance of blood colloidal osmotic pressure to the transport of hormones and bilirubin to the buffering of pH. One of the other important functions it serves is the transport of fatty acids in the blood. These molecules typically exhibit very low aqueous solubility, but association with HSA allows them to be solubilized up to 2 mM.[30] Serum albumin has also been widely investigated for its ability to interact with drug molecules that are administered intravenously. This interaction has been exploited in Abraxane, an FDA-approved oncology product that uses HSA to deliver paclitaxel. It is currently marketed for the treatment of non-small cell lung cancer, breast cancer, and pancreatic cancer.[31] Clinical trials are currently underway for a series of similar constructs, currently known as ABI-008 through ABI-010, which deliver docetaxel, rapamycin, and tanespimycin, respectively.[32] A recent investigation demonstrated that cancer vaccines can also be tethered to HSA, allowing delivery to lymph nodes.[33] The success of HSA as a carrier of anticancer drugs can be attributed to its nonimmunotoxicity, long circulation time in blood, and high tumor accumulation.[34,35] Although the interaction of platinum anticancer agents with HSA has been extensively investigated,[36−38] only recently have systems been designed to exploit HSA as a vehicle for delivering platinum agents. In one instance, a covalent bond was formed between the pendant maleimide of a Pt(IV) complex and the sole free cysteine thiol of HSA.[39]

We begin with an investigation of the effect of systematically increasing the chain length of the carbamate ligand of **4a−e** on cellular uptake and cytotoxicity. The most promising compound, **4e**, was investigated further for its ability to interact with HSA. The resulting non-covalent protein-platinum complex is highly robust and can be purified by fast protein liquid chromatography (FPLC), permitting its physical and biological properties to be examined. Finally, the stability of **4e** in blood was investigated by exploiting the change in lipophilicity that occurs on reduction from Pt(IV) to Pt(II). The results of these studies indicate that **4e** is orders of magnitude more stable in blood than previously investigated Pt(II) and Pt(IV) compounds and that its ability to interact with HSA may confer this stability.

RESULTS

Synthesis and Characterization. A series of amphiphilic Pt(IV) constructs was prepared using the synthetic approach shown in Scheme 1. Hydrogen peroxide oxidation of cisplatin (**1**) in water affords **2**. The asymmetrically functionalized Pt(IV) compound **3** can be obtained by reaction of **2** with succinic anhydride.[40] The fortuitous acetone solubility of the disuccinate compound and the insolubility of **3** provide an effective means of removing the undesired side product.[41] The ability of isocyanate reagents to undergo nucleophilic attack by the platinum-bound hydroxide ligand of **3**[42,43] was exploited to form a series of amphiphilic Pt(IV) carbamate species. In this series, compounds **4a−e** bear a hydrophobic unbranched aliphatic chain varying in length from C2 to C16. The pendant carboxylate of the succinate ligand trans to the carbamate was used for further functionalization as described below. The Pt(IV) compounds were fully characterized by multinuclear (^{1}H, ^{13}C, and ^{195}Pt) NMR spectroscopy and electrospray ionization mass spectrometry (ESI-MS) (Figures S1−S5 in the Supporting Information). In the ^{1}H NMR spectra of **4a−e**, an increase in the intensity of the resonant absorption from δ = 1.2−1.3 ppm arose due to the increasing number of methylene units in the carbamate chain. Across the series, little change was observed in the peaks at 2.3, 2.9, 6.5, and 6.6 ppm arising from the succinate CH_2CH_2 fragment, carbamate CH_2NHCO fragment, and ammine ligands. These compounds all display a ^{195}Pt NMR signal around δ = 1240 ppm, confirming the 4+ oxidation state of the platinum. In the ESI mass spectra, well-defined isotopic distribution patterns provided further confirmation of chemical composition. Chemical purity was established with combustion analysis and analytical HPLC (Figure S6 in the Supporting Information). The latter also provides information about the increase in hydrophobicity on transitioning from **4a** to **4e**. The compounds show systematically increasing retention on a C18 reverse-phase stationary phase as the length of the chain increases. The lipophilicity of the compounds can be directly evaluated by measuring the extent to which they partition between octanol and water, $P_{o/w}$ or simply P. Measured log P values are reported in Figure S8 in

dx.doi.org/10.1021/ja5038269 | J. Am. Chem. Soc. 2014, 136, 8790−8798

(a)

Cell Line	Cancer Type	IC_{50} (μM) cisplatin	**4a** (C2)	**4b** (C6)	**4c** (C8)	**4d** (C12)	**4e** (C16)	**7**
A549	Lung	3.83±0.21	55.0±3.24	20.9±1.10	19.03±1.62	1.22±0.34	0.41±0.04	-
A2780	Ovarian	1.86±0.14	45.3±4.41	7.02±0.28	4.80±0.39	0.30±0.04	0.16±0.04	0.12±0.01
A2780CP70	Ovarian[a]	6.49±1.4	91.2 ±13.9	18.4±0.64	7.86±1.85	0.27±0.04	0.10±0.02	0.13±0.01
Resistance[b]	-	3.48	2.01	2.62	1.64	0.90	0.62	1.1

a: Resistant to cisplatin; b: IC_{50}(A2780CP70)/ IC_{50}(A2780)

(b)

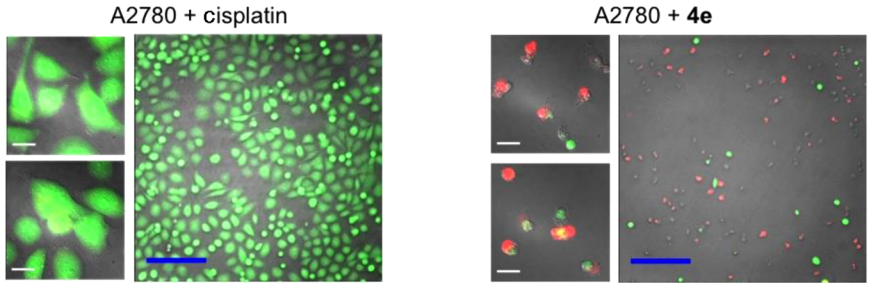

Figure 1. Cytotoxicity profiles of the Pt(IV) prodrugs: (a) table of measured IC_{50} values for **4a**−**e** and **7** in A549, A2780, and A2780CP70 cell lines; (b) calcein AM/ethidium homodimer-1 cell viability assay, details of which may be found in the main text and Supporting Information (white scale bar, 20 μm; blue scale bar, 200 μm).

the Supporting Information. As expected, the experimental log *P* values increased from **4a** (log *P* = −1.72 ± 0.21) to **4e** (log *P* = 1.23 ± 0.04). The log *P* values of these complexes were also calculated using the online program ALOGSP 2.143.[44] The calculated log *P* values are linearly proportional to the experimentally measured log *P* values (Figure S8 in the Supporting Information).

To study the reduction of this class of compounds, a coumarin molecule was attached to the pendant carboxylate of **4b** using standard amide-bond-formation chemistry to produce **5**. As with **4a**−**e**, multinuclear NMR and mass spectra are consistent with the formulation of the compound as shown in Figure S9 in the Supporting Information. The photophysical and chemical properties of this compound are discussed below.

Cytotoxicity Profiles. The in vitro anticancer activity of these newly synthesized Pt(IV) compounds was assessed by using the MTT assay. Three human cancer cell lines, namely, the non-small cell lung cancer cell line A549, ovarian cancer cell line A2780, and cisplatin-resistant ovarian cancer cell line A2780CP70, were evaluated. Cancer cells were treated with cisplatin or one of **4a**−**e** for 72 h and cell viability was evaluated. IC_{50} values, which represent the concentration required to inhibit growth by 50%, are given in Figure 1a. The in vitro anticancer activity of **4e**, the most potent member of the series, was also confirmed by using fluorescent microscopy and the LIVE/DEAD cell assay, a combination of the ethidium homodimer-1 assay and staining with acetomethoxycalcein, or calcein AM (Figure 1b). Live cells stain with calcein AM and yield a green fluorescence signal, whereas dead cells exhibit no fluorescence or a red signal due to the ethidium homodimer-1. A2780 ovarian cancer cells treated with 10 μM **4e** for 48 h were mostly dead, but those treated with cisplatin under the same conditions had mostly survived. The IC_{50} for cisplatin at 48 h is 6.35 ± 1.39 μM, and that for **4e** is 0.26 ± 0.04 μM. These cytotoxicity data agree with the observation in LIVE/DEAD cell assay. In addition, we further evaluated the cytoxicity of **4e** in normal human cells. The IC_{50} value of **4e** in the MRC-5 (normal lung tissue) cell line is 1.34 ± 0.13 μM, which is about 8 times higher than that in the A2780 ovarian cancer cell lines (IC_{50} = 0.16 ± 0.04 μM).

Cellular Uptake. The extent of cellular uptake was investigated by treating A2780 ovarian cancer cells with 5 μM of cisplatin or one of **4a**−**e** for 5 h. The whole cell concentration of platinum was then evaluated by graphite furnace atomic absorption spectroscopy (GFAAS). As expected, the results (Figure S11 in the Supporting Information) indicate that increase in chain length from C2, **4a**, to C16, **4e**, significantly enhances cellular uptake. The lead compound, **4e**, is taken up by the A2780 cells 160 times more effectively than **4a** and 40 times better than cisplatin. Notably, from **4a** to **4e**, the 160-fold increase in cellular uptake is mirrored by a 280-fold increase in cytotoxicity, suggesting that the increase in cytotoxicity can be attributed in large part to the increase in uptake. The subcellular distribution of **4e** was investigated and revealed that most of the platinum is present in the cytosol, indicating that, despite its lipophilic character, it does not become trapped in the membrane (Figure S12 in the Supporting Information).

Activation by Reduction. Given that Pt(IV) prodrugs are posited to undergo obligatory reduction prior to anticancer activity, we investigated the reduction of a cisplatin prodrug bearing axial succinate and carbamate ligands. Reduction of **5**, a fluorescent analogue of **4**, was evaluated using fluorescence spectroscopy (Figures S15−S17 in the Supporting Information). Compound **5** has a quantum yield (ϕ) of 0.047, and the succinyl-coumarin ligand alone, **6**, has a ϕ of 0.85 (Figure S16 in the Supporting Information). The emission of these two compounds is depicted in Figure S16b in the Supporting Information. Upon excitation at 365 nm, **5** exhibits no visible emission, whereas **6** has intense blue emission. Compound **5** shows no significant turn-on upon standing in PBS even after overnight incubation at 37 °C. When a 10 μM solution of **5** was treated with 10 equiv of ascorbic acid in PBS, the coumarin ligand began to detach within 4 h, as confirmed by analytical HPLC and fluorescence spectroscopy (Figure S17 in the Supporting Information).

dx.doi.org/10.1021/ja5038269 | J. Am. Chem. Soc. 2014, 136, 8790−8798

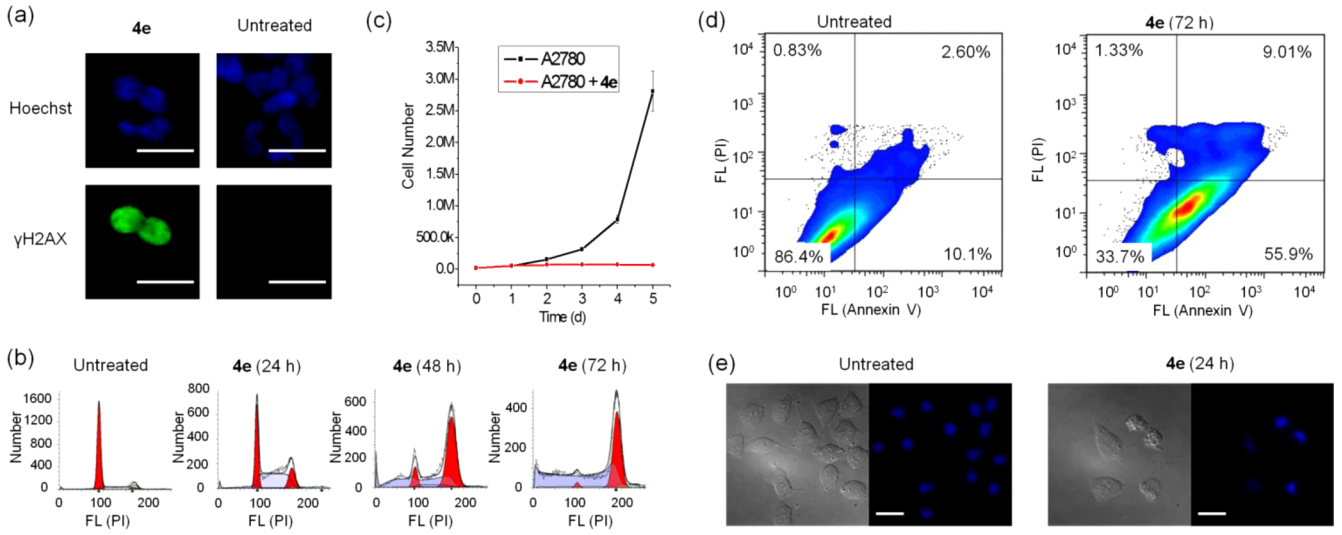

Figure 2. DNA damage and cellular responses of A2780 cells treated with **4e**: (a) immunostaining of the biomarker of DNA damage, phosphorylated H2AX (γH2AX) (scale bar, 20 μm); (b) flow cytometric analysis of cell cycle indicating that **4e** induced cell cycle arrest at the G2/M phase at 0.2 μM; (c) **4e** can inhibit proliferation in A2780 cells at 0.2 μM; (d) Annexin V/PI coupled flow cytometric analysis showing **4e** induced apoptosis in a large population of cells at 0.2 μM; (e) cellular images show characteristic apoptotic cell changes (blebbing, chromatin condensation, and nuclear fragmentation) upon treatment with 1 μM of **4e** for 24 h (scale bar, 20 μm).

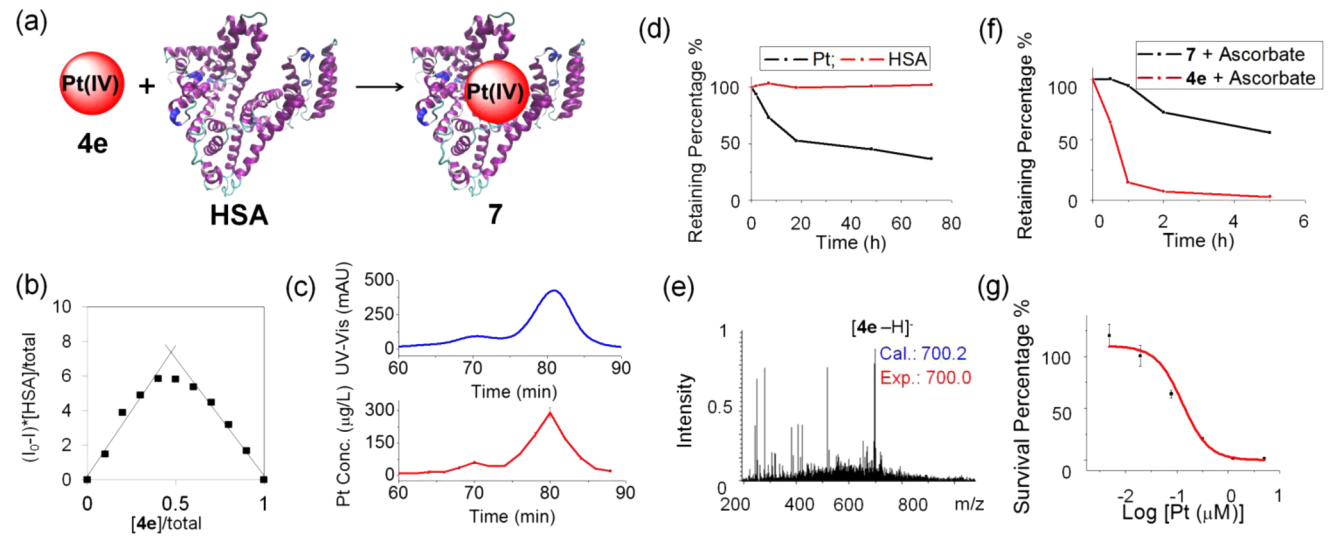

Figure 3. Systematic investigation of the Pt-HSA complex, **7**: (a) schematic representation of the formation of **7**; (b) Job plot of the Pt-HSA complex showing 1:1 stoichiometry; (c) FPLC trace of **7** and the corresponding GFAAS trace indicate that **4e** is tightly bound to HSA; (d) dialysis experiment indicating that around 60% of the platinum compound was released from **7** over 72 h and that the HSA is retained within the 3 kDa MWCO micro-dialysis bag; (e) ESI-mass spectrum of the octanol extract showing an intense signal at m/z = 700.1 for $[\mathbf{4e} - H]^-$ supporting the integrity of **4e** in **7**; (f) octanol extraction analysis showing that >90% of **4e** (3 μM) was reduced by ascorbate (30 μM) after 2 h incubation at 37 °C in the absence of HSA. The reduction was decreased to <50% by forming the Pt-HSA complex (3 μM); (g) cytotoxicity profile of **7** against A2780 human ovarian cancer cells showing an IC_{50} value of 0.12 ± 0.01 μM.

DNA Binding. DNA is the typical cellular target of cisplatin, and so the ability of **4** to platinate nuclear DNA was assessed. Five million A2780 cells were treated with growth medium containing 5 μM cisplatin, **4a**, or **4e** for 5 h, followed by incubation in fresh media for an additional 16 h. The intracellular DNA was isolated and the quantity of bound platinum was measured by GFAAS. The extent of DNA platination (Figure S18 in the Supporting Information) was determined to be 255 ± 55 Pt adducts/10^6 nucleotides for **4e**, 36.4 ± 5.5 Pt adducts/10^6 nucleotides for cisplatin, and 31.2 ± 4.1 Pt adducts/10^6 nucleotides for **4a**.

Biomarker of DNA Damage Caused by 4e. γH2AX, the phosphorylated form of histone protein H2AX, is a known biomarker of DNA damage caused by cisplatin.[45,46] γH2AX can be detected by immunoblotting and immunostaining. As shown in Figure 2a, fluorescence microscopy can be used to visualize the localization of γH2AX in the nucleus of A2780 cells treated with **4e**. Similarly, the phosphorylation of H2AX in A2780 cells treated with **4e** could also be observed by Western blotting (Figure S19 in the Supporting Information), indicative of genomic DNA damage.

Cellular Responses. DNA-flow cytometric studies were conducted to identify the incidence of cell cycle arrest following

dx.doi.org/10.1021/ja5038269 | J. Am. Chem. Soc. 2014, 136, 8790−8798

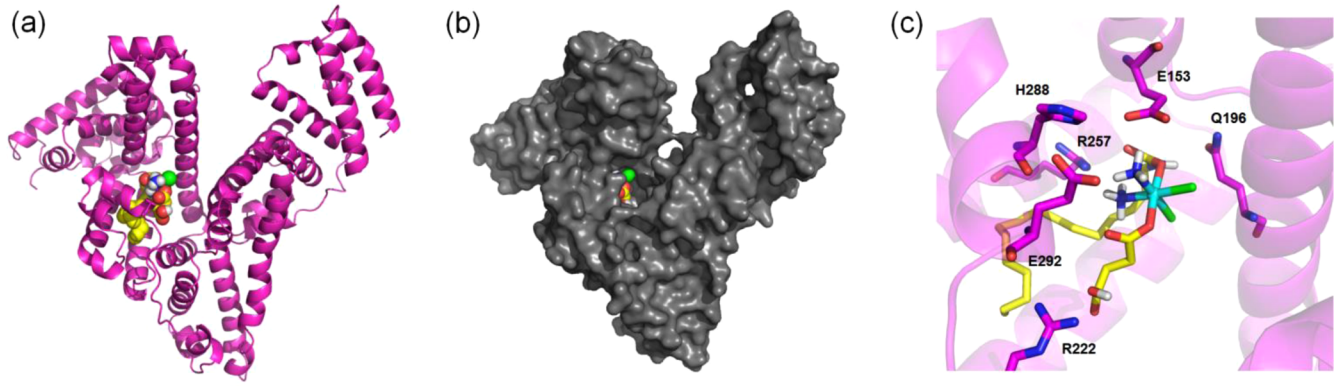

Figure 4. Docking studies of **4e** and HSA using Autodock Vina: (a) lowest energy structure; (b) platinum complex is buried beneath the protein surface; (c) platinum compound interacting with a variety of amino acid residues.

treatment with **4e**. As shown in Figure 2b, **4e** arrests the cycle in A2780 cells in a time-dependent manner. After 24 h incubation, a large proportion (66.5%) of cells accumulated at the S (51.1%) and G2/M (15.4%) phases. After 72 h incubation, cells were arrested at G2/M (96.5% of whole cell population). Cell proliferation experiments provide further evidence for the induction of cell cycle arrest by **4e**. As shown in Figure 2c, **4e** completely inhibits proliferation in A2780 cancer cells at concentrations as low as 0.2 μM. Using a dual staining annexin V/PI flow cytometry assay, the occurrence of apoptosis was studied in A2780 cells treated with **4e** (Figure 2d and Figure S20 in the Supporting Information). The results show that **4e** can efficiently induce apoptosis in A2780 cells after 72 h. Even at a low concentration of 0.2 μM, **4e** prompts a large population of cells to undergo early (55.9%) and late (9.07%) stage apoptosis. Apoptotic cells normally exhibit changes in cell morphology, such as blebbing, chromatin condensation, and nuclear fragmentation, all of which can be observed by fluorescence microscopy. A2780 cells treated with **4e** display a dose- and time-dependent morphological change (Figure S21 in the Supporting Information). As shown in Figure 2e, blebbing occurs following treatment of A2780 cells with 1 μM **4e** for 24 h. Chromatin condensation and nuclear fragmentation was also identified by Hoechst staining. All these cell-based experiments clearly indicate that **4e** can effectively induce DNA damage and thus lead to cell cycle arrest and apoptosis in cancer cells.

Interaction with Human Serum Albumin. Owing to the general similarity of the amphiphilic compounds **4a**–**e** to fatty acids, we hypothesized that they may be able to interact with HSA and take advantage of this association for transport in the blood (Figure 3a). The binding affinity of HSA (Sigma-Aldrich, A1887) toward **4a**, **4d**, and **4e** was investigated by using fluorescence spectroscopy. Specifically, fluorescence quenching of the Trp214 residue caused by the Pt(IV) complexes was measured (Figure S22 in the Supporting Information). The compound bearing a C16 hydrophobic chain, **4e**, displayed the highest affinity, with a binding constant (K_a) of 1.04×10^6 M^{-1}. Compound **4d** exhibited weaker binding ($K_a = 3.7 \times 10^4$ M^{-1}), whereas **4a** bound poorly ($K_a = 2.6 \times 10^3$ M^{-1}). Analysis of a Scatchard plot (Figure S22 in the Supporting Information) revealed a 1:1 binding ratio between **4e** and HSA, further supported by a Job plot (Figure 3b). In PBS, the concentration of **4e** at saturation is 3 μM, but upon complexation with HSA to form **7**, Pt concentrations of up to 400 μM can be achieved. An FPLC analysis was carried out to characterize **7**. The features of the UV–vis trace of **7** are similar to those of pure HSA, implying that binding of **4e** leads to minimal structural changes in the protein (Figure S23 in the Supporting Information). Moreover, the features of the Pt trace of **7**, representing the Pt content in the fractions of effluent as measured by GFAAS, match well those of the UV–vis trace (Figure 3c), suggesting that **4e** is tightly bound to HSA. A comparison of the UV–vis and GFAAS data reveals that **4e** and HSA associate in a 1.1:1 ratio to form **7**. This result is consistent with the 1:1 ratio obtained from the fluorescence studies (vide supra). Release of **4e** from **7** was evaluated by dialysis of a PBS solution of the construct against water. A 10 μM solution of **7** in PBS was loaded into a 3 kDa MWCO micro-dialysis bag and, as shown in Figure 3d, ~60% of the platinum compound was released after 72 h at room temperature. The nonpolar nature of **4e** permits facile extraction of the complex from aqueous solutions into octanol. Over 90% of the platinum compound can be extracted from an aqueous solution of **7** in this manner, as determined by GFAAS (Figure S24 in the Supporting Information). The molecular identity of the species extracted into octanol was confirmed by ESI-MS (Figure 3e).

Reduction of 4e and 7. Upon reduction, the hydrophobic Pt(IV) compound **4e** (log P = 1.23) produces a hydrophilic Pt(II) product, cisplatin (log P = −2.19), which is scarcely extracted into octanol. Therefore, by measuring the Pt content in an octanol extract of a mixture of products of reduction of **4e**, the degree of reduction can be established. Reduction of **4e** by ascorbate was evaluated using this method. Two different concentrations (30 μM and 300 μM) of ascorbate were used, corresponding to the concentrations found in blood and the intracellular environment, respectively. Compound **4e** (3 μM) is readily reduced by ascorbate at both low and high concentrations (Figure 3f and Figure S25 in the Supporting Information). After 2 h incubation at 37 °C, >90% of **4e** is reduced. In a separate experiment, a 3 μM solution of **7** exhibited much slower reduction of the Pt(IV) species after similar treatment. Even after **7** is incubated with reductant for 5 h (Figure 3f), more than 50% of the platinum remains as the hydrophobic Pt(IV) species.

Cytotoxicty of 7. MTT assays were carried out to assess the cytotoxicity of **7** (Figures 1a and 3g). Complex **7** isolated by FPLC exhibits comparable cytotoxicity to **4e** in ovarian cancer cell lines A2780 and A2780CP70 (IC_{50} = 0.12 ± 0.01 μM against A2780 and IC_{50} = 0.13 ± 0.01 μM against

dx.doi.org/10.1021/ja5038269 | J. Am. Chem. Soc. 2014, 136, 8790–8798

A2780CP70). These data represent a 60-fold improvement in efficacy over that of cisplatin.

Molecular Modeling. Docking studies were conducted to further investigate the non-covalent interaction between **4e** and HSA to form 7. The HSA protein scaffold from 1E7H was used in a broad search for interactions of **4e**. Of the top nine strongest interactions found, six place the platinum complex in the same pocket. This pocket, located in subdomain IIA, is known as Sudlow's site I and has been previously identified as a locus of drug interaction with HSA.[47,48] The lowest energy structure is shown in Figure 4a. The platinum complex is buried beneath the protein surface (Figure 4b). The more polar fragments of the molecule, which lie closer to the platinum center, interact with a variety of amino acid residues (Figure 4c). Specifically, Arg233 interacts with the pendant carboxylate of the succinate. Glu292, Glu153, and His288 are in close proximity to the ammine ligands bound to the Pt. Arg257 is directed toward the carbamate carbonyl, and Gln169 is positioned above the carbamate fragment. The lipophilic C16 tail is coiled into a hydophobic channel lined by Tyr150, Leu238, Leu219, Leu234, Phe223, Ile264, Ala261, Ile290, and Tyr150. The Pt(IV) center is located approximately 1 nm away from Trp214, allowing for quenching of the fluorescence from the tryptophan residue, which is consistent with the fluorescence studies described above.

Stability of the 4e in Whole Human Blood. The stability of Pt(IV) prodrugs in blood is critically important for their application in clinical settings. We therefore investigated the stability of **4e** in whole human blood by exploiting the ability of octanol to selectively extract unreduced **4e** from aqueous solution. Compound **4e** (60 μM) was incubated in fresh whole human blood at 37 °C. After 0, 1, 2, 4, and 7 h, aliquots were extracted with octanol to remove the remaining Pt(IV) complex. The Pt content in the octanol extract was measured using GFAAS, and the structural integrity of the extracted material was confirmed using analytical HPLC. As shown in Figure 5, the Pt content of the octanol extract decreases to 49%

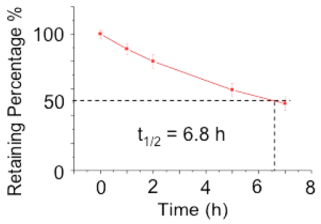

Figure 5. Stability of **4e** in whole human blood showing a half-life of 6.8 h.

after 7 h incubation. HPLC analysis (Figure S26 in the Supporting Information) indicates that the extracted Pt species is indeed **4e** by comparison with pure material. This result reveals the half-life of **4e** in fresh whole human blood to be 6.8 h.

DISCUSSION

Pt(IV) Prodrugs with Similarity to Fatty Acids. It can be appreciated that the structures of **4a**–**e** bear an overall likeness to those of fatty acids. Although molecular similarity can be rigorously defined,[49] the metrics typically employed are unsuitable in this particular instance given that there is no meaningful set of dissimilar compounds with which to contrast this similarity. Like fatty acids, **4a**–**e** have an overall amphiphilic nature due to the presence of a long hydrophobic chain and a terminal carboxylic acid (Scheme 1). Compounds **4a**–**e** were readily synthesized by employing validated chemical reactions, providing access to this class of previously unreported Pt(IV) prodrugs bearing *trans* carbamate and carboxylate axial ligands.

The lipophilicity of this set of compounds, directly evaluated by measuring log *P*, could be readily tuned simply by increasing the length of the aliphatic chain of the carbamate ligand. An increase in the length of the chain, and consequently in the lipophilicity, led to a systematic increase in cytotoxicity from 1 order of magnitude lower to almost 2 orders of magnitude higher than that of cisplatin.[50] This phenomenon was observed in all three of the cell lines tested (Figure 1a). The lead compound of the series, **4e**, which bears a C16 hydrophobic chain, exhibited the most potent in vitro anticancer activity. In all three of the cell lines tested, the cytotoxicity of **4e** is substantially greater (9–70 times) than that of cisplatin (Figure 1a). As shown in Figure 1a, **4e** also displays a lower resistance factor in ovarian cancer cell lines than cisplatin or **4a**–**d**. The activity of **4e** is demonstrated by staining cells with calcein AM and ethidium, the so-called LIVE/DEAD cell assay. In this assay, treatment with cisplatin or **4e** at equimolar concentrations led to drastically different degrees of cell survival.

A likely source of this increased potency lies in the greater ability of lipophilic compounds to traverse the plasma membrane. As expected, cellular uptake of the platinum compounds **4** by A2780 cancer cells increases as the length of the carbamate chain increases. As suggested in a recent report, cellular uptake of Pt(IV) compounds is highly related to their in vitro activity.[51] Plotting log [IC_{50} (μM)] vs log [uptake (pmol Pt/million cells)], reveals the linear relationship between the two (R^2 = 0.98) depicted in Figure 6a. A plot of log [uptake (pmol Pt/million cells)] vs log *P* (Figure 6b) also exhibits a

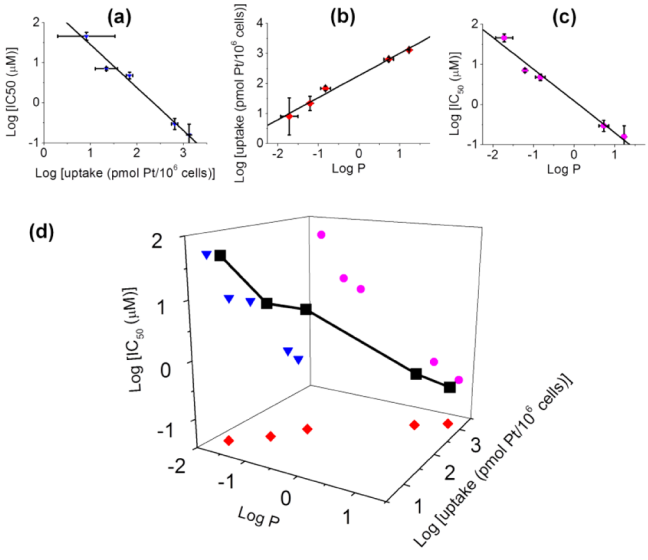

Figure 6. Structure–activity relationship of **4a**–**e** between hydrophobicity (log *P*), cytotoxicity (IC_{50}), and cellular uptake in A2780 cells: (a) 2D correlation of cytotoxicity of the platinum(IV) complexes and their cellular uptake (b) 2D correlation of cellular uptake and hydrophobicity; (c) 2D correlation of hydrophobicity and cytotoxicity; (d) 3D plot of hydrophobicity, cytotoxicity, and cellular uptake (black squares). The projections shown in the various planes are the corresponding 2D plots (parts a–c).

dx.doi.org/10.1021/ja5038269 | J. Am. Chem. Soc. 2014, 136, 8790–8798

linear relationship (R^2 = 0.99). The anticipated linear relationship also occurs between log P and log [IC_{50} (μM)] (Figure 6c), confirming that hydrophobicity directly contributes to the cytotoxicity of these complexes. Using these three factors, a 3D structure−activity plot was constructed (Figure 6d). The graph clearly establishes a three-way relationship between hydrophobicity, cellular uptake, and cytotoxicity.

Mechanism of Action. After entry into cells, Pt(IV) prodrugs are activated by reduction.[10] Reaction of **4a**−**e** with intracellular reductants such as glutathione or ascorbic acid will release cisplatin, which subsequently conveys anticancer activity. Use of fluorescence methods to detect the reduction of Pt(IV) species in biological environments has attracted much recent attention.[52−55] In order to investigate the redox behavior of **4a**−**e**, we prepared a coumarin-conjugated Pt(IV) compound, **5**, which displays a significant increase in fluorescence intensity upon reduction. The similarity between the coordination spheres and ^{195}Pt NMR chemical shifts of **4a**−**e** and **5** indicate that the metal-centered redox properties of the latter are relevant in assessing those of the former. In **5**, the fluorescence of the coumarin fluorophore is quenched owing to the heavy atom effect induced by platinum. Upon reduction, the coumarin-containing ligand is released, as determined by HPLC, resulting in enhanced fluorescence. Using **5**, it was possible to ascertain that Pt(IV) constructs of the type **4a**−**e** can be reduced by biologically relevant concentrations of ascorbate within hours. Following such reductive activation, **4a**−**e** exert their anticancer activity via the released cisplatin. This active Pt(II) moiety induces cell death by forming DNA cross-links. Accordingly, DNA from A2780 cells that had been treated with **4a**−**e** contained amounts of platinum roughly proportional to the cytotoxicity of the compound, and phorphorylation of H2AX, a biomarker of DNA damage, was detected in the same cell line following treatment with **4e**. The mechanism of action of **4a**−**e** was further probed by analyzing the influence of treatment with the platinum agent on the progression of cells through the cell cycle. Platination is recognized by the cell as DNA damage, which induces cell cycle arrest. If the damage cannot be repaired, cells are signaled to commit apoptosis. The observation of G2/M arrest following S phase arrest is consistent with the known response of cells to cisplatin treatment.[1] Cisplatin activates the G2/M checkpoint, allowing DNA to be repaired before mitosis and at the same time preventing cisplatin-damaged DNA from being inherited by daughter cells. The induction of apoptosis was confirmed by the annexin V/propidium iodide (PI) assay. In healthy cells, phosphatidylserine (PS) is located on the cytoplasmic surface of the cell membrane. In apoptotic cells, PS is translocated from the inner to the outer surface of the plasma membrane, exposing PS to the external cellular environment where it can be detected by annexin V conjugates. Combining annexin V and PI, both early and late stage apoptosis can be identified. Indeed, **4e**, the most potent member of the series, induces a large population of cells to enter into early and late stage apoptosis. The morphological changes that are expected to accompany apoptosis, such as blebbing and chromatin condensation, were also observed.

Interaction with HSA. The amphiphilic structure of compounds **4a**−**e** mimics that of the fatty acids that are naturally transported by HSA. We therefore investigated the interaction of the most potent complex, **4e**, with this protein. The fluorescence of Trp214, the sole tryptophan in the protein, is quenched by the heavy atom effect when a platinum complex approaches it via association with HSA. The quenching is complete within a few seconds of adding the platinum complex, before acquisition of the first fluorescence measurement. This phenomenon can be used to create a Job plot, which reveals that **4e** associates with HSA in a 1:1 stoichiometry. Isolation of the protein by FPLC and quantification of the amount of protein and platinum in this species confirms the 1:1 molar ratio. The nature of the interaction between the two is proposed to be non-covalent because extraction of an aqueous solution of **7** with octanol removes **4e** from HSA in a nearly quantitative manner. ESI-MS measurements on the octanol extract confirm the molecular identity of **4e** in the non-polar phase.

The 1:1 stoichiometry implies that a specific non-covalent interaction may be occurring between **4e** and HSA. Molecular docking simulations were used to investigate possible binding sites for **4e** on the protein. The lowest energy binding site coincides with Sudlow's site I.[47,48] This pocket has been classically associated with drug binding and is one of the sites to which fatty acids bind.[56] As can be seen in Figure 4, the platinum complex is buried beneath the protein surface when bound in this pocket. This feature suggests that association with HSA may slow biological reduction of the Pt(IV) center by preventing reductants from forming an activated complex with the anticancer prodrug.

The influence of HSA complexation on the reduction of **4e** was probed by exploiting the high lipophilicity of this platinum complex. As described above, extraction of an aqueous solution of **7** is able to completely remove **4e** from the protein. Compound **4e** was added to whole human blood and incubated at 37 °C. The platinum complex rapidly associates with HSA to form **7** in situ. At various time points an aliquot of the platinated blood was extracted with octanol. The Pt(IV) species with its axial lipophilic carbamate is extracted into the octanol, whereas the hydrophilic cisplatin, produced by reduction, is not. Quantification of the platinum extracted into octanol at each time point therefore provides a measure of the rate of reduction in blood. HPLC analysis of the octanol phase confirms that **4e** is the extracted species. The half-life of **4e** in blood obtained from these measurements is 6.8 h, which is significantly greater than that of cisplatin ($t_{1/2}$ = 21.6 min) or satraplatin ($t_{1/2}$ = 6.3 min).[28,57] These favorable chemical properties combine with the inherent nonimmunogenicity, biocompatibility, and enhanced tumor accumulation of HSA to produce a system that holds significant therapeutic potential.

Rapid association between **4e** and HSA, in conjunction with the high concentration of the latter in blood, suggests that injection of **4e** as a small molecule agent will result in the rapid in situ formation of **7**. We envisage, however, that for practical reasons **4e** would be better formulated as **7** and administered as the protein-platinum complex. This approach permits much higher concentrations of **4e** to be solubilized in water and eliminates the need to administer **4e** using organic cosolvents or additives.

■ CONCLUSION

In conclusion, we presented the successful development of a novel Pt(IV) prodrug, **4e**, that is capable of associating with serum albumin to form a Pt:HSA construct, **7**. Compound **4e** was obtained from the study of a series of amphiphilic Pt(IV) complexes designed to mimic the structure of fatty acids. By tuning length of the hydrophobic chain present in these compounds, cytotoxicity could be modulated from an order

dx.doi.org/10.1021/ja5038269 | J. Am. Chem. Soc. 2014, 136, 8790−8798

magnitude lower to almost 2 orders of magnitude greater than that of cisplatin. The lead compound, **4e**, exhibits excellent in vitro anticancer activity, showing 9−70 times better activity than cisplatin in lung and ovarian cancer cell lines. Investigation of the fluorophore-bearing anolog, **5**, confirmed that the prodrugs described here interact with biological reductants, lose axial ligands on conversion to Pt(II), and subsequently platinate DNA. As a consequence of the DNA damage, cell cycle arrest and apoptosis were observed. A strong non-covalent interaction between **4e** and HSA permits the formation and isolation of **7**, which can act as a delivery vehicle for **4e**. This interaction with HSA protects **4e** in the reducing environment of the blood. This interaction contributes to the promising stability of **4e** in whole human blood. **4e** shows a 6.8 h half-life in whole human blood, which is significantly longer than that of cisplatin ($t_{1/2} \sim$ 20 min) or satraplatin ($t_{1/2} \sim 6$ min).

MATERIALS AND METHODS

General Procedure for the Synthesis of Compounds 4. Compound **3** was placed into a 5 mL glass vial and an anhydrous DMF solution (2 mL) of the corresponding isocyanate was added. The suspension was stirred overnight. The next day, the suspension had become a clear green solution. The solution was then filtered and the solvent was removed under reduced pressure at 65 °C. Ethyl ether (2 mL) was added to the oily residue, and the mixture was ultrasonicated for 1 min and centrifuged. The solid was further washed with DCM (4 mL) and diethyl ether (2 mL). The washed solid was then left under vacuum overnight.

Synthesis of 4a. Reagents used in the reaction: Compound **3** (200 mg, 0.468 mmol), ethyl isocyanate (70 mg, 0.945 mmol). Yield: 162 mg (68.6%). ^{1}H NMR (400 MHz, DMSO-d_6): δ: 6.51 (m, 7H, NH3 and $NH_{carbamate}$), 2.89 (q, 2H, C*H2*CH3), 2.34 (m, 4H, succinate), 0.94 (t, 3H, CH2C*H3*). ^{13}C NMR (100 MHz, DMSO-d_6): δ: 180.2, 174.3, 164.2, 36.0, 31.0, 30.4, 15.9. ^{195}Pt NMR (86 MHz, DMSO-d_6): 1239.8. ESI-MS (negative mode) for $C_7H_{17}Cl_2N_3O_6Pt$: $[M - H]^-$, calcd m/z 504.0; found, 503.9. Anal. Calcd for $C_7H_{17}Cl_2N_3O_6Pt$: C, 16.64; H, 3.39; N, 8.32. Found: C, 17.08; H, 3.27; N, 7.98.

Synthesis of 4b. Reagents used in the reaction: Compound **3** (50 mg, 0.117 mmol), hexyl isocyanate (30 mg, 0.236 mmol). Yield: 37.6 mg (57%). ^{1}H NMR (400 MHz, DMSO-d_6): δ: 6.51 (m, 7H, NH3 and $NH_{carbamate}$), 2.85 (q, 2H, C*H2*(CH2)4CH3), 2.34 (m, 4H, succinate), 1.22 (m, 8H, CH2(C*H2*)4CH3), 0.85 (t, 3H, CH2-(CH2)4C*H3*).^{13}C NMR (100 MHz, DMSO-d_6): δ: 184.5, 174.4, 164.2, 41.5, 31.6, 30.9, 30.4, 30.3, 26.6, 22.6, 14.4. ^{195}Pt NMR (86 MHz, DMSO-d_6): 1242.3. ESI-MS (negative mode) for $C_{11}H_{25}Cl_2N_3O_6Pt$: $[M - H]^-$, calcd m/z 560.1; found, 560.0. Anal. Calcd for $C_{11}H_{25}Cl_2N_3O_6Pt$: C, 23.54; H, 4.49; N, 7.49. Found: C, 23.52; H, 4.21; N, 7.36.

Synthesis of 4c. Reagents used in the reaction: Compound **3** (100 mg, 0.234 mmol), octyl isocyanate (80 mg, 0.515 mmol). Yield: 60.8 mg (44.2%). ^{1}H NMR (400 MHz, DMSO-d_6): δ: 6.51 (m, 7H, NH3 and $NH_{carbamate}$), 2.87 (q, 2H, C*H2*(CH2)6CH3), 2.35 (m, 4H, succinate), 1.22 (m, 12H, CH2(C*H2*)6CH3), 0.85 (t, 3H, CH2-(CH2)6C*H3*).^{13}C NMR (100 MHz, DMSO-d_6): δ: 180.0, 174.3, 164.4, 41.5, 31.7, 30.9, 30.4, 30.3, 29.3, 29.2, 26.9, 22.6, 14.4. ^{195}Pt NMR (86 MHz, DMSO-d_6): 1240.7. ESI-MS (negative mode) for $C_{13}H_{29}Cl_2N_3O_6Pt$: $[M - H]^-$, calcd, m/z 588.1; found, 588.0. Anal. Calcd for $C_{13}H_{29}Cl_2N_3O_6Pt$: C, 26.49; H, 4.96; N, 7.13. Found: C, 26.15%; H, 4.51; N, 6.99.

Synthesis of 4d. Reagents used in the reaction: Compound **3** (50 mg, 0.117 mmol), dodecyl isocyanate (50 mg, 0.237 mmol). Yield: 76.7 mg (68.8%). ^{1}H NMR (400 MHz, DMSO-d_6): δ: 6.50 (m, 7H, NH3 and $NH_{carbamate}$), 2.87 (q, 2H, C*H2*(CH2)10CH3), 2.36 (m, 4H, succinate), 1.23 (m, 20H, CH2(C*H2*)10CH3), 0.85 (t, 3H, CH2-(CH2)10C*H3*).^{13}C NMR (100 MHz, DMSO-d_6): δ: 180.0, 174.3, 164.4, 41.5, 31.8, 30.9, 30.4, 30.3, 29.6, 29.5, 29.5, 29.4, 29.3, 29.2, 26.9, 22.6, 14.4. ^{195}Pt NMR (86 MHz, DMSO-d_6): 1240.3. ESI-MS (negative mode) for $C_{17}H_{37}Cl_2N_3O_6Pt$: $[M - H]^-$, calcd, m/z 644.2; found, 644.1. Anal. Calcd for $C_{17}H_{37}Cl_2N_3O_6Pt$: C, 31.63; H, 5.78; N, 6.51. Found: C, 31.48; H, 5.25; N, 6.40.

Synthesis of 4e. Reagents used in the reaction: Compound **3** (50 mg, 0.117 mmol), hexadecyl isocyanate (69 mg, 0.258 mmol). Yield: 32.7 mg (39.9%). ^{1}H NMR (400 MHz, DMSO-d_6): δ: 6.51 (m, 7H, NH3 and $NH_{carbamate}$), 2.87 (q, 2H, C*H2*(CH2)14CH3), 2.35 (m, 4H, Succinate), 1.23 (m, 28H, CH2(C*H2*)14CH3), 0.85 (t, 3H, CH2(CH2)14C*H3*).^{13}C NMR (100 MHz, DMSO-d_6): δ: 180.0, 174.4, 164.4, 41.5, 31.8, 31.0, 30.4, 30.3, 29.5, 29.5, 29.2, 26.9, 22.6, 14.5. ^{195}Pt NMR (86 MHz, DMSO-d_6): 1240.4. ESI-MS (negative mode) $C_{21}H_{45}Cl_2N_3O_6Pt$: $[M - H]^-$, calcd, m/z 700.2; found, 700.1. Anal. Calcd for $C_{21}H_{45}Cl_2N_3O_6Pt$: C, 35.95; H, 6.46; N, 5.99. Found: C, 35.72; H, 6.02; N, 5.61.

ASSOCIATED CONTENT

Supporting Information

Experimental details regarding the characterization of **4a−e** and **5**, cell culture, the MTT assay, fluorescence studies, FPLC analysis, immunoblotting, immunostaining, molecular modeling, and blood stability tests. This material is available free of charge via the Internet at http://pubs.acs.org.

AUTHOR INFORMATION

Corresponding Author

lippard@mit.edu

Notes

The authors declare the following competing financial interest(s): S.J.L. has a financial interest in Blend Therapeutics.

ACKNOWLEDGMENTS

This work was supported by National Cancer Institute Grant CA34992. We also thank the Kathy and Curt Marble Cancer Research Fund (Y.-R.Z. and S.J.L.), a Misrock Postdoctoral Fellowship to K.S., CCNE, the Samsung Foundation of Culture for a Samsung Scholarship and the CCNE graduate support for the CCNE grant (5 U54 CA151884) to H.Y., and MIT UROP Office support to J.G.B. Spectroscopic instrumentation at the MIT DCIF is maintained with funding from NIH Grant 1S10RR13886-01.

REFERENCES

(1) Wang, D.; Lippard, S. J. *Nat. Rev. Drug Discovery* **2005**, *4*, 307.
(2) Kelland, L. *Nat. Rev. Cancer* **2007**, *7*, 573.
(3) Wheate, N. J.; Walker, S.; Craig, G. E.; Oun, R. *Dalton Trans.* **2010**, *39*, 8113.
(4) Jamieson, E. R.; Lippard, S. J. *Chem. Rev.* **1999**, *99*, 2467.
(5) Todd, R. C.; Lippard, S. J. *Metallomics* **2009**, *1*, 280.
(6) Miller, R. P.; Tadagavadi, R. K.; Ramesh, G.; Reeves, W. B. *Toxins* **2010**, *2*, 2490.
(7) Hall, M. D.; Hambley, T. W. *Coord. Chem. Rev.* **2002**, *232*, 49.
(8) Hall, M. D.; Dolman, R. C.; Hambley, T. W. In *Metal Complexes in Tumor Diagnosis and as Anticancer Agents*; Sigel, A., Sigel, H., Eds.; Metal Ions in Biological Systems, Vol. *42*; Marcel Dekker: New York, 2004; p 297.
(9) Hall, M. D.; Mellor, H. R.; Callaghan, R.; Hambley, T. W. *J. Med. Chem.* **2007**, *50*, 3403.
(10) Johnstone, T. C.; Wilson, J. J.; Lippard, S. J. *Inorg. Chem.* **2013**, *52*, 12234.
(11) Shamsuddin, S.; Santillan, C. C.; Stark, J. L.; Whitmire, K. H.; Siddik, Z. H.; Khokhar, A. R. *J. Inorg. Biochem.* **1998**, *71*, 29.
(12) Hambley, T. W.; Battle, A. R.; Deacon, G. B.; Lawrenz, E. T.; Fallon, G. D.; Gatehouse, B. M.; Webster, L. K.; Rainone, S. *J. Inorg. Biochem.* **1999**, *77*, 3.
(13) Khan, S. R. A.; Huang, S.; Shamsuddin, S.; Inutsuka, S.; Whitmire, K. H.; Siddik, Z. H.; Khokhar, A. R. *Bioorg. Med. Chem.* **2000**, *8*, 515.

(14) Gramatica, P.; Papa, E.; Luini, M.; Monti, E.; Gariboldi, M. B.; Ravera, M.; Gabano, E.; Gaviglio, L.; Osella, D. *J. Biol. Inorg. Chem.* **2010**, *15*, 1157.
(15) Mukhopadhyay, S.; Barnés, C. M.; Haskel, A.; Short, S. M.; Barnes, K. R.; Lippard, S. J. *Bioconjugate Chem.* **2008**, *19*, 39.
(16) Graf, N.; Mokhtari, T. E.; Papayannopoulos, I. A.; Lippard, S. J. *J. Inorg. Biochem.* **2012**, *110*, 58.
(17) Barnes, K. R.; Kutikov, A.; Lippard, S. J. *Chem. Biol.* **2004**, *11*, 557.
(18) Ang, W. H.; Khalaila, I.; Allardyce, C. S.; Juillerat-Jeanneret, L.; Dyson, P. J. *J. Am. Chem. Soc.* **2005**, *127*, 1382.
(19) Dhar, S.; Lippard, S. J. *Proc. Natl. Acad. Sci. U.S.A.* **2009**, *106*, 22199.
(20) Yang, J.; Sun, X.; Mao, W.; Sui, M.; Tang, J.; Shen, Y. *Mol. Pharmaceutics* **2012**, *9*, 2793.
(21) Suntharalingam, K.; Song, Y.; Lippard, S. J. *Chem. Commun.* **2014**, *50*, 2465.
(22) Dhar, S.; Gu, F. X.; Langer, R.; Farokhzad, O. C.; Lippard, S. J. *Proc. Natl. Acad. Sci. U.S.A.* **2008**, *105*, 17356.
(23) Dhar, S.; Kolishetti, N.; Lippard, S. J.; Farokhzad, O. C. *Proc. Natl. Acad. Sci. U.S.A.* **2011**, *108*, 1850.
(24) Johnstone, T. C.; Lippard, S. J. *Inorg. Chem.* **2013**, *52*, 9915.
(25) Xu, X.; Xie, K.; Zhang, X.-Q.; Pridgen, E. M.; Park, G. Y.; Cui, D. S.; Shi, J. J.; Wu, J.; Kantoff, P. W.; Lippard, S. J.; Langer, R.; Walker, G. C.; Farokhzad, O. C. *Proc. Natl. Acad. Sci. U.S.A.* **2013**, *110*, 18638.
(26) Li, J.; Yap, S. Q.; Chin, C. F.; Tian, Q.; Yoong, S. L.; Pastorin, G.; Ang, W. H. *Chem. Sci.* **2012**, *3*, 2083.
(27) Chaney, S. G.; Wyrick, S.; Till, G. K. *Cancer Res.* **1990**, *50*, 4539.
(28) Carr, J. L.; Tingle, M. D.; McKeage, M. J. *Cancer Chemother. Pharmacol.* **2002**, *50*, 9.
(29) *A.D.A.M. Medical Encyclopedia*; A.D.A.M., Inc.: Atlanta, GA, 2005; Vol. *2014*.
(30) Voet, D.; Voet, J. G. *Biochemistry*, 4th ed.; John Wiley & Sons: Hoboken, NJ, 2011.
(31) Hawkins, M. J.; Soon-Shiong, P.; Desai, N. *Adv. Drug Delivery Rev.* **2008**, *60*, 876.
(32) Vishnu, P.; Roy, V. *Breast Cancer: Basic Clin. Res.* **2011**, 53.
(33) Liu, H.; Moynihan, K. D.; Zheng, Y.; Szeto, G. L.; Li, A. V.; Huang, B.; Van Egeren, D. S.; Park, C.; Irvine, D. J. *Nature* **2014**, *507*, 519−522.
(34) Kratz, F. *J. Controlled Release* **2008**, *132*, 171.
(35) Park, K. *J. Controlled Release* **2012**, *157*, 3.
(36) Ivanov, A. I.; Christodoulou, J.; Parkinson, J. A.; Barnham, K. J.; Tucker, A.; Woodrow, J.; Sadler, P. J. *J. Biol. Chem.* **1998**, *273*, 14721.
(37) Espósito, B. P.; Najjar, R. *Coord. Chem. Rev.* **2002**, *232*, 137.
(38) Timerbaev, A. R.; Aleksenko, S. S.; Polec-Pawlak, K.; Ruzik, R.; Semenova, O.; Hartinger, C. G.; Oszwaldowski, S.; Galanski, M.; Jarosz, M.; Keppler, B. K. *Electrophoresis* **2004**, *25*, 1988.
(39) Pichler, V.; Mayr, J.; Heffeter, P.; Dömötör, O.; Enyedy, É. A.; Hermann, G.; Groza, D.; Köllensperger, G.; Galanksi, M.; Berger, W.; Keppler, B. K.; Kowol, C. R. *Chem. Commun.* **2013**, *49*, 2249.
(40) Dhar, S.; Daniel, W. L.; Giljohann, D. A.; Mirkin, C. A.; Lippard, S. J. *J. Am. Chem. Soc.* **2009**, *131*, 14652.
(41) Wilson, J. J.; Lippard, S. J. *Chem. Rev.* **2014**, *114*, 4470.
(42) Giandomenico, C. M.; Abrams, M. J.; Murrer, B. A.; Vollano, J. F.; Rheinheimer, M. I.; Wyer, S. B.; Bossard, G. E.; Higgins, J. D., III *Inorg. Chem.* **1995**, *34*, 1015.
(43) Wilson, J. J.; Lippard, S. J. *Inorg. Chem.* **2011**, *50*, 3103.
(44) Tetko, I. V.; Tanchuk, V. Y. *J. Chem. Inf. Comput. Sci.* **2002**, *42*, 1136.
(45) Olive, P. L.; Banáth, J. P. *Cytometry, Part B* **2009**, *76B*, 79.
(46) Revet, I.; Feeney, L.; Bruguera, S.; Wilson, W.; Dong, T. K.; Oh, D. H.; Dankort, D.; Cleaver, J. E. *Proc. Natl. Acad. Sci. U.S.A.* **2011**, *108*, 8663.
(47) Sudlow, G.; Birkett, D. J.; Wade, D. N. *Mol. Pharmacol.* **1975**, *11*, 824.
(48) Sudlow, G.; Birkett, D. J.; Wade, D. N. *Mol. Pharmacol.* **1976**, *12*, 1052.
(49) *Concepts and Applications of Molecular Similarity*; Johnson, M. A., Maggiora, G. M., Eds.; Wiley: New York, 1990.
(50) Braddock, P. D.; Connors, T. A.; Jones, M.; Khokhar, A. R.; Melzack, D. H.; Tobe, M. L. *Chem.−Biol. Interact.* **1975**, *11*, 145.
(51) Reithofer, M. R.; Bytzek, A. K.; Valiahdi, S. M.; Kowol, C. R.; Groessl, M.; Hartinger, C. G.; Jakupec, M. A.; Galanski, M.; Keppler, B. K. *J. Inorg. Biochem.* **2011**, *105*, 46.
(52) New, E. J.; Duan, R.; Zhang, J. Z.; Hambley, T. W. *Dalton Trans.* **2009**, 3092.
(53) Wilson, J. J.; Lippard, S. J. *Inorg. Chim. Acta* **2012**, *389*, 77.
(54) Song, Y.; Suntharalingam, K.; Yeung, J. S.; Royzen, M.; Lippard, S. J. *Bioconjugate Chem.* **2013**, *24*, 1733.
(55) Montagner, D.; Yap, S. Q.; Ang, W. H. *Angew. Chem., Int. Ed.* **2013**, *52*, 11785.
(56) Curry, S.; Mandelkow, H.; Brick, P.; Franks, N. *Nat. Struct. Biol.* **1998**, *5*, 827.
(57) Erdlenbruch, B.; Nier, M.; Kern, W.; Hiddemann, W.; Pekrun, A.; Lakomek, M. *Eur. J. Clin. Pharmacol.* **2001**, *57*, 393.